



# QUANTUM INTERNET ALLIANCE

# **D3.4 Report on generation of telecom photon with ion compatible spectrum from solid-state quantum memories**

## Document History

Revision Nr	Description	Author	Review	Date
1	First draft	Hugues de Riedmatten, Soeren Wengerowsky		21.12.2021

*This project has received funding from the European Union's Horizon 2020 research and innovation programme under grant agreement No 820445.*

*The opinions expressed in this document reflect only the author's view and in no way reflect the European Commission's opinions. The European Commission is not responsible for any use that may be made of the information it contains.*

# Index

1. Abstract .....	5
2. Keyword list.....	5
3. Acronyms & Abbreviations .....	5
4. Introduction .....	6
5. Entangled photon-pair source with embedded solid-state quantum memory .....	7
6. Quantum frequency conversion of micro-second long photons from 606 nm to telecom wavelength.....	9
6.1. Initial results.....	10
6.2. Results with NTT waveguide .....	11
7. Conclusion .....	12
8. References.....	13

## 1. Abstract

Interfacing quantum repeater nodes and quantum processing nodes is an important capability to scale up quantum network. In QIA, one of the proposed connection is between the Praseodymium doped crystal quantum memory at 606 nm developed by ICFO and a single trapped Ca ion from the University of Innsbruck. The bandwidth of the trapped ion is around 100 kHz, which requires the creation and frequency conversion of single photons with several microsecond duration from the solid-state node. In this deliverable, we summarize the efforts done at ICFO for creating long single photons from a solid-state quantum memory, and for converting microsecond long photons from 606 nm to 1550 nm.

## 2. Keyword list

Quantum Frequency conversion, solid-state quantum memory, single trapped ion

## 3. Acronyms & Abbreviations

<b>DoA</b>	Description of Action
<b>EC</b>	European Commission
<b>WP</b>	Work Package
<b>AFC</b>	Atomic frequency comb
<b>SW</b>	Spin wave
<b>DLCZ</b>	Duan-Lukin-Cirac-Zoller
<b>QFC</b>	Quantum Frequency Conversion

## 4. Introduction

One of the important capability required to scale up quantum networks, and indeed one of the important long term goals of QIA, is to transfer quantum information between quantum repeater nodes and quantum processing nodes. One possibility is to directly transfer qubits between the nodes using a single photon as carrier. This is very challenging because the to types of nodes typically interact with photons at different wavelengths and with different temporal waveforms. One of the proposed connection within QIA is between the solid-state quantum repeater node based on Praseodymium doped solids developed at ICFO and the quantum processing node based on single trapped Ca ion in a cavity developed at the University of Innsbruck (UIBK) and IQOQI (see Fig. 1). The connection between the two photons would happen via a photon at telecommunication wavelength. The bandwidth of the trapped ion is very narrow, of order of 100 kHz<sup>1</sup>, which poses significant challenges in terms of photon generation and conversion. In this deliverable, we will describe work done at ICFO towards the generation of a telecom photon with an ion compatible spectrum and its conversion to telecom wavelength.

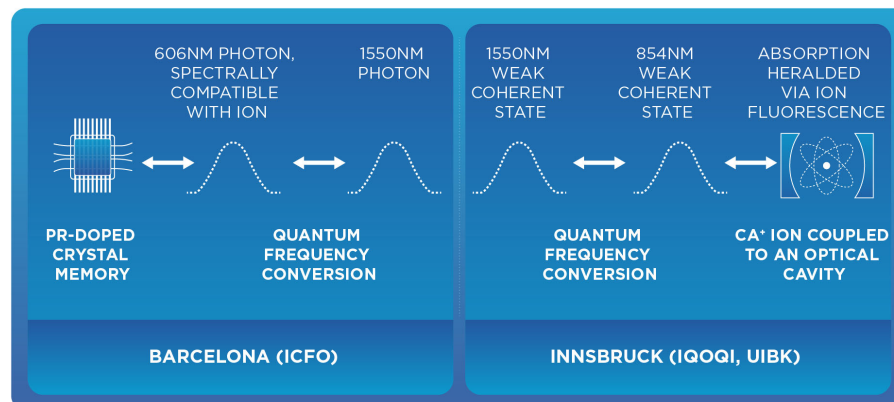


**Figure 1:** Scheme of the proposed interface between a solid-state quantum memory and single trapped ion via a photon at telecom wavelength.

There are two main challenges associated with our objective. The first challenge is to develop an efficient source of ultra-narrowband single photons with widely tunable temporal waveform using our crystal quantum memory, to create the photons with the required bandwidth (100 kHz) and temporal waveform for efficient interaction with the single trapped ion. The second challenge is to efficiently frequency convert this long photon at 606 nm to the telecom band with low added noise, such that it could in principle be sent to a distant single trapped ion for heralded absorption.

The work at ICFO was divided into two parts, addressing the two challenges: (1) the generation of long single photons from a Pr quantum memory and (2) the quantum frequency conversion of us long weak coherent states mimicking single photons. In the next chapters we describe the work performed along these two directions.

## 5. Entangled photon-pair source with embedded solid-state quantum memory

ICFO has demonstrated a solid-state entangled photon pair source with an embedded quantum memory<sup>2</sup>. In this source, the detection of a photon heralds the presence of a collective spin excitation in the quantum memory, which after a variable storage time can be read-out and converted into a single photon.

A very convenient method to directly generate light-matter entanglement in atomic ensembles is the Duan-Lukin-Cirac-Zoller (DLCZ) protocol<sup>3</sup>. It is based on the off-resonant excitation by means of weak classical write pulses of an atomic ensemble with a lambda system. With a small probability, a Raman scattered write photon creates a collective spin excitation, heralded by the emission of a Stokes photon. The spin wave can be converted into a second photon, the anti-Stokes photon, with the use of a strong on-resonant read pulse. The DLCZ protocol has been very successfully implemented in cold atomic gases. However, the standard off resonant DLCZ scheme is difficult to apply to rare-earth ion doped crystals, due to the very weak dipole moments of the optical transition. Alternative schemes have been proposed that use resonant excitation and rephasing techniques to counteract the inhomogeneous dephasing of the atomic dipoles.

ICFO's source is based on the combination of the atomic frequency comb and the Duan-Lukin-Cirac-Zoller scheme using a  $\text{Pr}^{3+}:\text{Y}_2\text{SiO}_5$  crystal solid-state quantum memory. The experimental setup and the relevant level scheme is shown in Fig. 1. The write pulse is sent in resonance with the AFC created in the crystal. The detection of an initial Stokes photon heralds the presence of a single spin wave stored in the crystal, which can then be read-out on demand, emitting a single photon time-bin qubit. The retrieved single photon has a duration has a duration of 700 ns (FWHM), corresponding to a linewidth of 630 kHz.

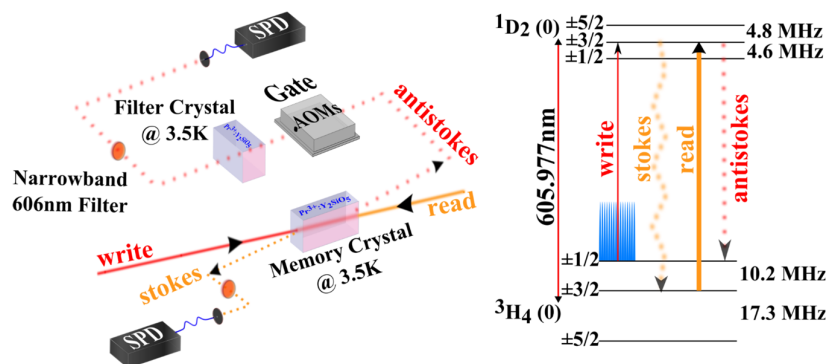
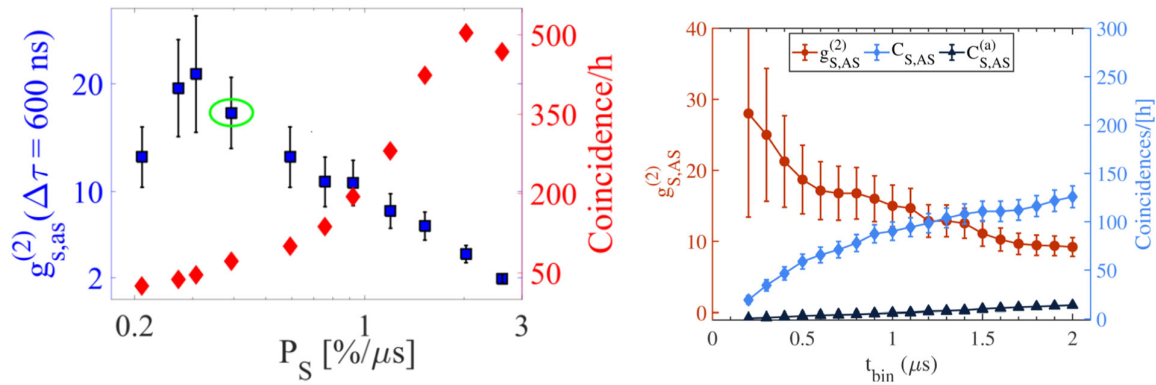


Figure 2. Left, Experimental setup. Right: Level scheme Pr:YSO

The source has been characterized by measuring the second-order cross-correlation function  $g_{s,as}^{(2)}$ , as a function of the probability to generate a Stokes photon (see Fig. 3). We reached  $g_{s,as}^{(2)}$  values up to 20 for a coincidence window of 600 ns, strongly in the quantum regime. The coincidence count rate was increased by a factor of 8 compared to a previous demonstration by ICFO<sup>4</sup>. In addition, we have also demonstrated a violation of Bell inequalities with the emitted photons.



**Figure 3.** Left: Measurement of second order cross correlations (blue squares) and coincidence count rate (red diamond) for the photon pairs emitted by the quantum memory as a function of the probability to generate a Stokes photon. Right: Second order cross correlation (red), coincidences and accidental coincidences as a function of the coincidence detection window.

The read-out efficiency is currently of the order of 2 %. This value could be increased by suppressing background noise in the Stokes photon emission, by improving the AFC preparation, by a better control of the spin decoherence as well as by using a longer crystal with higher optical depth and/or by embedding the crystal in a low finesse cavity<sup>5</sup>. Furthermore, background noise suppression would also allow us to widen the coincidence window, leading to a higher coincidence rate, as show in Fig. 3.

We have designed and built a cavity, which is now operative and incorporated in our memory setup, and we have recently improved the efficiency of an excited state AFC quantum memory up to 63 %, the highest value measured so far for an AFC memory<sup>6</sup> (for a more detailed description, see Deliverable D2.1). Investigations are ongoing to extend cavity enhanced storage to spin-waves and we also plan to combine the impedance matched cavity with AFC-DLCZ generation. We also expect that the bandwidth of the retrieved photon can be decreased to a value around close to 100 kHz (photon duration around 4-5 microseconds), a value compatible with a single trapped ion, by using longer write/read pulses and improving the atomic frequency comb generation.

## 6. Quantum frequency conversion of micro-second long photons from 606 nm to telecom wavelength

We used a periodically poled Lithium Niobate buried waveguide (HC photonics) to perform difference frequency generation (DFG) with a pump Laser (Toptica TA pro, amplified with Toptica BoosTA) of 994 nm. Energy conservation ensures the wavelength of the generated photons to be 1552 nm:  $\frac{1}{1552} = \frac{1}{606} - \frac{1}{994}$ .

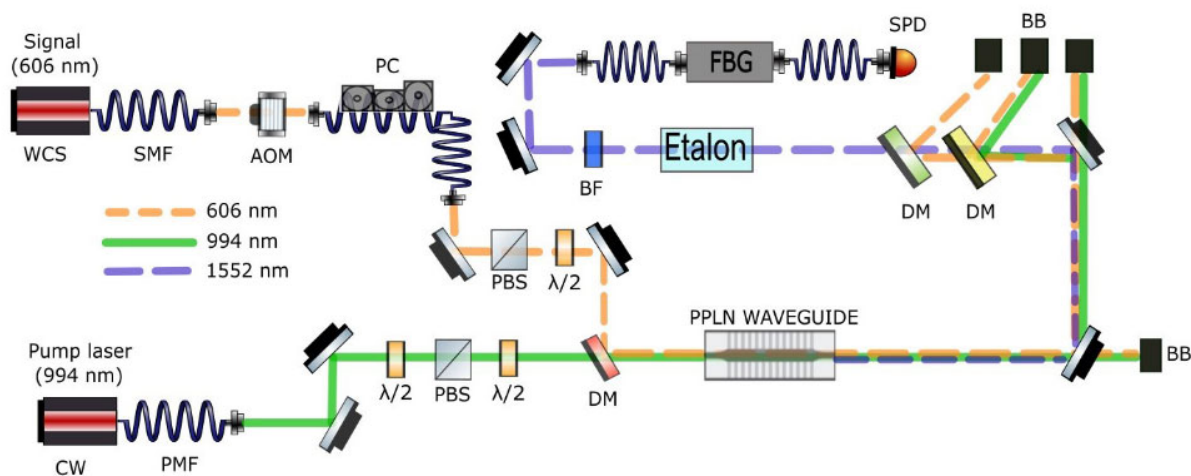


**Figure 4: Scheme of the setup:** The Gaussian-shaped weak coherent state (WCS) at 606 nm is created by an arbitrary-waveform-generator and an acousto-optic modulator (AOM) using a cavity-locked 606 nm laser of a bandwidth around 1 kHz. The CW pump beam and the signal beam are overlapped and coupled through the temperature-stabilized ppLN waveguide. Afterward, the pump and signal are filtered out in order to isolate the converted signal. The etalon, band-pass filter (BF) and fiber bragg grating (FBG) help to suppress the SPDC noise around the signal.

Abbreviations: WCS: continuous wave; AOM: acousto-optic modulator; PC: manual polarisation controller; PBS: polarising beam-splitter; DM: dichroic mirror; SMF: single-mode fiber; PM: polarisation-maintaining fiber;  $\lambda/2$ : half-wave plate; BF: band-pass filter; FBG: fiber bragg-grating; SPD: single photon avalanche detector (ID230).

The setup for quantum frequency conversion is displayed in Figure 1. In order to test the setup, Gaussian pulses were shaped with an arbitrary-waveform generator and an acousto-optic modulator (AOM) using a cavity-locked 606 nm laser of a bandwidth of around 1 kHz. The wavelength of 606 nm is compatible with Praseodymium-based quantum memories.

The signal is filtered spectrally by means of an etalon with a bandwidth of 210 MHz, a 6 nm dielectric band-pass-filter (BF) and a fiber-bragg grating (FBG) of 2.5 GHz bandwidth.

The quantum frequency conversion of single photons with a duration of around 200 ns has been realized in our group and reported by Maring et al<sup>7</sup>. However, the conversion of microsecond long photons compatible with the Ca trapped ion has not been demonstrated yet. Reaching high-signal to noise ratio allowing high-fidelity conversion is challenging

for long photons because the amount of detected noise scales linearly with the duration of the time-window considered. Moreover, the conversion of single photons emitted by the DLCZ-AFC quantum memory with high signal-to-noise ratio is very challenging because the current read-out efficiency from the quantum memory is around 2 %, meaning that in the current conditions, pulses with at most 0.02 photons will reach the quantum frequency converter conditioned on the detection of a Stokes photon. To reach a signal to noise ratio  $> 10$ , as desirable for quantum communication will therefore require high efficiency and ultra-low noise frequency conversion. The relevant figure of merit is the  $\mu_1$  parameter, which corresponds to the number of input photons to reach a signal to noise ratio of 1 at the output of the converter and should therefore be as small as possible.

## 6.1. Initial results

A first set of measurements was performed with a 1.4 cm long ridge PPLN waveguide from the company HC-Photonics. A measurement of  $\mu_1$  as a function of the pulse duration can be seen in Figure 5. With this waveguide we could achieve a  $\mu_1$  value of  $0.05/\mu\text{s}$ . For the single photons emitted by our quantum memory, which have a duration of 700 ns, the corresponding  $\mu_1$  value is about 0.03 which is still too large to convert signals of about 0.02 photons per pulse with high SNR. For photon durations of 4  $\mu\text{s}$  (corresponding to a frequency bandwidth of 110 kHz), the  $\mu_1$  is around 0.2. The device efficiency achieved with this waveguide was about 9% (including all the filtering system), while the internal efficiency was about 40%, measured via the depletion of the signal. While reaching high signal-to-noise ratios with 1 us long photons would still be possible in case the read-out efficiency of the quantum memory could be greatly improved, the achieved  $\mu_1$  value would allow a maximum SNR of around 5 for 4 us long photons, even in the ideal case of unity memory read-out efficiency. In order to achieve larger SNRs, we have considered two solutions: the use of a new more efficient waveguide, and the use of narrower frequency filters. In the next section, we show preliminary results with a new waveguide.

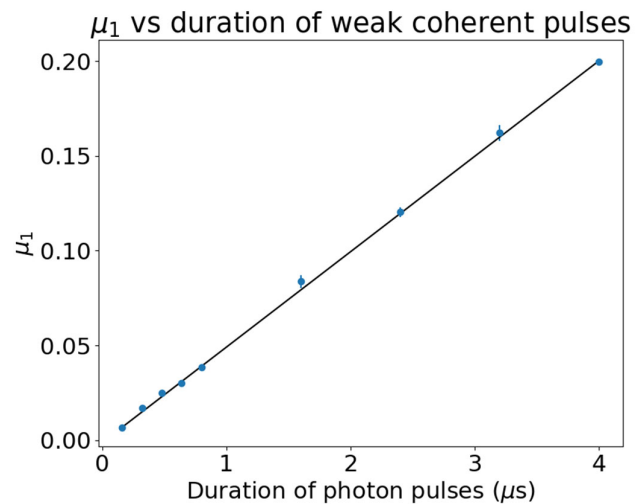


Figure 5: Measurement of  $\mu_1$  as a function of the pulse duration for the HCP waveguide. The input number was adjusted in order to send the same number of input photons for each pulse length. The pump power was 533 mW in front of the waveguide.

## 6.2. Results with NTT waveguide

In order to improve both the signal-to-noise ratio and facilitate the conversion of photons with a duration over one microsecond, we simultaneously aim at both increasing the efficiency and reducing the noise. A 48 mm-long ridge waveguide from NTT has been purchased which has proven to show a good performance in recent publications<sup>8</sup>.

### Efficiency

The new waveguide has shown to have a higher efficiency of  $(790 \pm 40) \%W/cm^2$ . This efficiency is approximately 8 times higher than that of the previously used waveguides. This higher efficiency also comes with a higher internal efficiency over 80%, measured by observing the signal depletion, and a device efficiency of over 27%, which is the ratio between the number of 606 nm photons observed before the waveguide and the number of photons observed after the FBG, measured with classical detectors in CW. This is more than three times as high as the values observed with the former waveguide which was used by Maring et al.

### Noise Level

We also performed preliminary measurement of conversion of weak coherent pulses to infer the  $\mu_1$  value for the NTT waveguide. The higher device efficiency, together with a lower noise leads to a strong decrease in  $\mu_1$ , down to  $(1.1 \pm 0.5) \cdot 10^{-3}$  for pulses of 180 ns duration (FWHM). This corresponds to a  $\mu_1$  of  $6.1 \cdot 10^{-3}/\mu s$ , leading to a maximum SNR of 164 for a 1  $\mu s$  long pulse containing one single photon. This is an improvement by a factor around 8 compared with the HCP waveguide. The data can be seen in figure 6. For this measurement, the parameter  $\mu_1$ , is obtained by measuring the number of photons per pulse in front of the waveguide using a silicon SPAD (60% detection efficiency) and dividing it by the SNR of the detected converted telecom photons. Note that for this preliminary measurement the device efficiency of the setup was about 21.5%, lower than the maximum value

of 27% that we have observed in other measurements, such that there is room to improve the results. More measurement will be taken with this new waveguide in the coming weeks, but the preliminary results are already very

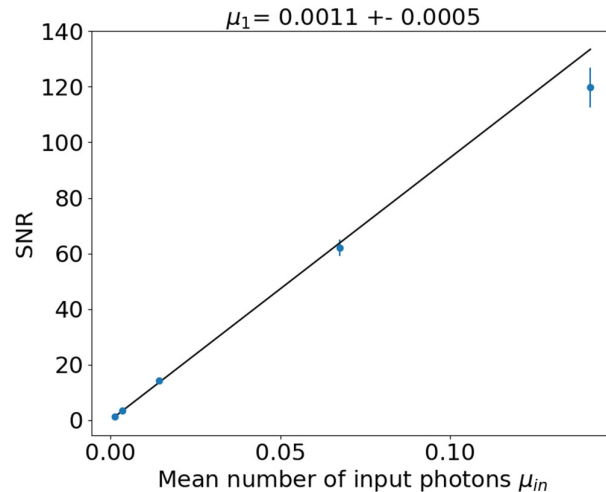


**Figure 6:** Measurement of  $\mu_1$ : The signal-to-noise ratio was measured for different mean photon numbers  $\mu_{in}$ .  $\mu_1$  is calculated as the inverse of the slope. This was obtained for a pulse length of 180 ns and a pump power of 200 mW in front of the waveguide. The window to collect the signal was twice the FWHM of the pulse: 360 ns.

promising. Extending the measured  $\mu_1$  to the 700 ns long photons emitted by our AFC-DLCZ memory leads to a  $\mu_1$  value of  $4.3 \cdot 10^{-3}$ , which would allow a conversion with SNR around 4.6 for the single photons, even with the currently low read-out efficiency.

Besides increasing the efficiency, another way to increase the SNR is to decrease the noise, which is currently dominated by weakly phase-matched SPDC from the pump laser<sup>9</sup>. This process is broadband and therefore a good way to reduce it is to use more narrow band filters. We plan to replace the fiber Bragg grating by a filter cavity with a linewidth of 20 MHz and a finesse of 100. In addition to being a 10-fold narrower spectral filter, the free spectral range is chosen to not align the modes with the etalon, such that large parts of the current etalon transmission will also be blocked. This effect will, presumably reduce the noise level and the  $\mu_1$  by at least one order of magnitude. Removing the fiber Bragg grating may also increase the device efficiency, as this filter only yields a transmission of about 60%. We have designed the filter cavity and plan to incorporate it in the setup in the coming months.

## 7. Conclusion

We have investigated the possibility and made important steps towards the realization of a quantum interface between solid-state quantum memories based on praseodymium doped crystals and single trapped Ca ions in a high-finesse cavity. In particular, we have studied the generation of long single photons with spectral bandwidth compatible with single trapped Ca ions from the solid-state quantum memory, and we have investigated the quantum frequency conversion of microsecond long photons from 606 nm to 1550 nm. We have demonstrated a solid-state entangled photon pair source with embedded quantum memory, able to generate single photons with a bandwidth of 630 kHz, and discussed the possibilities to reduce the bandwidth to 100 kHz, a value compatible with trapped ions. We have also demonstrated ultra-low noise quantum frequency conversion of weak coherent pulses with micro-second duration from 606 nm to 1550 nm, with a  $\mu_1$  value of  $6.1 \cdot 10^{-3} / \mu\text{s}$ . These results are promising and show that a quantum interface linking solid-state quantum memories and single ions is possible.

## 8. References

- <sup>1</sup> J. Schupp, V. Krcmarsky, V. Krutyanskiy, M. Meraner, T. E. Northup, B. P. Lanyon, Phys.Rev.X Quantum 2, 020331 (2021)
- <sup>2</sup> K. Kutluer, E. Distanto, B. Casabone, S. Duranti, M. Mazzera, and H. de Riedmatten, Phys. Rev. Lett. 123, 030501 (2019)
- <sup>3</sup> L.M. Duan, M. Lukin, J.I. Cirac and P. Zoller, Nature 414, 413 (2001)
- <sup>4</sup> K. Kutluer, M. Mazzera, and H. de Riedmatten Phys. Rev. Lett. 118, 210502 (2017)
- <sup>5</sup> M. Afzelius and C. Simon, Phys. Rev. A 82, 022310 (2010)
- <sup>6</sup> S. Duranti, S. Wengerowski, A.Seri, B.Casabone, H.de Riedmatten, in preparation (2022)
- <sup>7</sup> N. Maring, D. Lago-Rivera, A. Lenhard, G. Heinze, and H. de Riedmatten, Optica 5, 507 (2018)
- <sup>8</sup> P. Strassmann et al. Opt Express. 13;27(10):14298 (2019)
- <sup>9</sup> J. Pelc et al, Opt. Lett. **35**, 2804-2806 (2010)